ANNALS OF
BOTANY
Founded 1887

PART OF A SPECIAL ISSUE ON FUNCTIONAL–STRUCTURAL PLANT MODELLING

Modelling the development and arrangement of the primary vascular structure in plants

Fabrizio Cartenì[1],*, Francesco Giannino[1], Fritz Hans Schweingruber[2] and Stefano Mazzoleni[1]

[1]*Dipartimento di Agraria, University of Naples Federico II, via Università 100, 80055 Portici (Na), Italy and* [2]*Swiss Federal Institut of Forest, Snow and Landscape Research WSL, CH- 8903 Birmensdorf, Switzerland*
* For correspondence. E-mail fabrizio.carteni@unina.it

• **Background and Aims** The process of vascular development in plants results in the formation of a specific array of bundles that run throughout the plant in a characteristic spatial arrangement. Although much is known about the genes involved in the specification of procambium, phloem and xylem, the dynamic processes and interactions that define the development of the radial arrangement of such tissues remain elusive.
• **Methods** This study presents a spatially explicit reaction–diffusion model defining a set of logical and functional rules to simulate the differentiation of procambium, phloem and xylem and their spatial patterns, starting from a homogeneous group of undifferentiated cells.
• **Key Results** Simulation results showed that the model is capable of reproducing most vascular patterns observed in plants, from primitive and simple structures made up of a single strand of vascular bundles (protostele), to more complex and evolved structures, with separated vascular bundles arranged in an ordered pattern within the plant section (e.g. eustele).
• **Conclusions** The results presented demonstrate, as a proof of concept, that a common genetic–molecular machinery can be the basis of different spatial patterns of plant vascular development. Moreover, the model has the potential to become a useful tool to test different hypotheses of genetic and molecular interactions involved in the specification of vascular tissues.

Key words: Functional–structal plant modelling, reaction–diffusion, activator–substrate, pattern formation, morphogenesis, stele, primary vascular structure, phloem, xylem differentiation.

INTRODUCTION

During growth of plant axial organs, the process of vascular development takes place in two specific regions located directly below the shoot and root apical meristems. Such developmental processes result in the formation of a specific array of vascular bundles that run throughout the plant in a characteristic spatial arrangement. One of the first events in plant development that precedes the differentiation of the provascular tissues (as well as other tissues) is the establishment of polarity with the differential expression of patterning genes along both the apical–basal and the central–peripheral axes. Considering the radial patterning alone, the juxtaposition of the central and peripheral domains is thought to drive cotyledon and leaf outgrowth (Waites *et al.*, 1998) as well as providing a direct input in the radial patterning of vascular bundles (Carlsbecker and Helariutta, 2005).

Two distinct levels of spatial organization can be distinguished within the vascular system (Esau, 1977): a longitudinal pattern, i.e. the array of vascular bundles within an organ; and a radial pattern, which is the spatial arrangement of phloem and xylem within each vascular bundle and, more generally, within a transversal plant section. For the scope of our work, we will concentrate our attention on the radial pattern of plant stems and roots. In such a context, new procambium, phloem and xylem are consistently differentiated in a specific spatial pattern that varies between organs and species. The combination

of the vascular tissues of stems and roots with any other associated fundamental or ground tissue, such as pith and interfascicular regions, is defined the 'stele' or the 'central cylinder' (Esau, 1977). Beck *et al.* (1982) listed several types of recognized steles and classified them into three basic types: (1) protostele presenting a solid column of vascular tissue; (2) siphonostele characterized by a hollow cylinder of vascular tissue; and (3) eustele showing separated strands of vascular tissue, usually arranged as a discontinuous cylinder.

Much attention has been paid to hormonal (Bowman and Floyd, 2008; Vanstraelen and Benková, 2012) and genetic (Caño-Delgado *et al.*, 2010) control of developmental events and in particular to the role of auxin polar transport in the patterning of developing organs (Blilou *et al.*, 2005; Teale *et al.*, 2006), somehow ignoring the stimuli responsible for its involvement. Recent work on arabidopsis roots provided new insights into the mechanisms controlling vascular patterning. Bishopp *et al.* (2011*a*, *b*) investigated the roles of auxin and cytokinin in specifying and maintaining the radial patterning of xylem cells, identifying the feedback loop network between hormonal signalling and transport. On the other hand, phloem is established through asymmetric cell divisions followed by differentiation. A Myb family transcription factor, APL, has been identified as promoting such developmental events (Bonke *et al.*, 2003). In *apl* mutants, xylem differentiates in place of phloem cells and,

interestingly, when *APL* is ectopically expressed, the differentiation of xylem precursors is suppressed. Evidence from studies on arabidopsis mutants (Eshed *et al.*, 2001; Kerstetter *et al.*, 2001) shows that ectopic expression of *KANADI* genes results in abaxialized organs that do not develop any vasculature. These results suggested the antagonistic role of *HD-ZIP III* and *KANADI* genes and that the establishment of both adaxial/central and abaxial/peripheral domains is needed for the correct development of vascular tissues (Ilegems *et al.*, 2010).

In the late 1970s, Wilson (1978) proposed a hypothesis, based on experimental evidence, for the differentiation of vascular tissues in regenerating cambia involving opposing gradients of auxin and sucrose. Recently, new studies highlighted the possible interplay between sugar and auxin in plant growth and development (reviewed in Eveland and Jackson, 2012). Searching for genes expressed during the first stages of leaf development, Pien *et al.* (2001) found five genes showing a specific spatial pattern of expression within apical meristems. Interestingly, three of those genes encoded enzymes involved in sugar metabolism, providing evidence that carbohydrate metabolism is also spatially regulated during key developmental processes.

In the last decades, simulation models have proven to be useful tools to unravel the often non-intuitive relationships between local processes and the emergence of global forms and patterns (Jönsson and Krupinski, 2010). Several studies using computational modelling have been carried out on plant morphodynamics (reviewed in Prusinkiewicz and Runions, 2012), and recent work (reviewed in: Jönsson *et al.*, 2012) has focused on two topics: (1) venation and phyllotaxis driven by auxin polar transport and (2) genetic regulation of stem cells in apical meristems (Fujita *et al.*, 2011). In particular, modelling studies on vascular development mainly concentrated on the role of auxin in leaf venation. The first model was formulated by Sachs (1969), proposing the so-called 'canalization hypothesis'. According to this model, auxin export through a cell wall promotes further transport in the same direction, thus creating canals of preferential flow as a self-organization property of the system. Based on this hypothesis, many molecular models were formulated (e.g. Mitchison, 1980; Feugier *et al.*, 2005; Bayer *et al.*, 2009) and tested against experimental data (e.g. Scarpella *et al.*, 2006). A recently published work (Muraro *et al.*, 2014) based on the work of Bishopp *et al.* (2011*a*) presents a simulation model providing useful insights into the signalling network behind the radial patterning of procambium and xylem in arabidopsis root.

Apart from the work of Muraro *et al.* (2014), there has been no modelling effort as yet to study the radial patterning of primary vascular structures, i.e. the specification and spatial organization of procambium, phloem and xylem. Moreover, as far as we know, there are no published models able to simulate the diversity of steles observed in nature. In this study, we present a spatially explicit reaction–diffusion model inspired by the pioneering works of Turing (1953) and Meinhardt (1982). Our model defines a set of logical and functional rules able to simulate the differentiation of procambium, phloem and xylem, and the emerging radial patterns of vascular tissues. The model qualitatively reproduces most stelar structures observed in different plant taxa, demonstrating, as a proof of concept, that a common genetic–molecular machinery can be the basis of vascular development and patterning.

METHODS

Model description

We assume that a concentration gradient of a morphogenetic factor is established within plant meristems, which is interpreted by cells as a positional cue to initiate the definition of the central and peripheral domains. The ensuing differentiation of vascular cells strictly depends on the establishment of the radial patterning. In particular, the juxtaposition of central and peripheral domains is assumed to be indispensible for procambium definition and to provide positional cues for the specification of phloem and xylem. Scattered evidence is available on the spatial processes involved in the specification of procambium. Auxin seems to regulate the initiation of procambial cells during early embryo development. In the absence of auxin signalling mediated by MONOPTEROS (MP), an auxin-responsive factor, procambial cells do not form properly (Hardtke and Berleth, 1998). Wilson (1978) proposed the hypothesis that two morphogens, centrifugally diffusing auxin and centripetally diffusing sucrose, were responsible for the positioning of regenerating cambium after wounding. Based on these pieces of evidence, we assume that the activation of genes involved in procambium differentiation requires the presence of two different substances with opposing gradients. Moreover, phloem and xylem tissues are always found associated with one another and arranged in consistent patterns within each organ. It is possible to assume that the genes and molecules responsible for their differentiation somehow inhibit each other locally (meaning that a single cell can only become either phloem or xylem), but also facilitate each other laterally so that both tissues can differentiate at the same time. These assumptions are supported by the antagonistic role of HD-ZIP IIIs and KANADIs in the determination of adaxial–abaxial organ polarity and the regulation of vascular tissues specification (Emery *et al.*, 2003), and also by the evidence on the effects of APL on phloem and xylem differentiation (Bonke *et al.*, 2003). For the sake of simplicity, we used reaction–diffusion formulations that could adequately mimic the general behaviour of the above-mentioned interactions.

Based on such premises, we implemented a mathematical model that simulates the development of a group of undifferentiated cells in a sub-apical transverse section of stems and roots (Fig. 1). The model is composed of three groups of partial differential equations (PDEs), each module describing a set of developmental events leading to the differentiation of vascular tissues.

Spatial domain definition. The first equation describes the dynamics of the first morphogenetic signalling factor, S_0 within each cell. Its production is assumed to be a linear function of the distance from the centre of the section (d), while its consumption is due to a constant rate μ_{S_0}. So, we can write:

$$\frac{\partial S_0}{\partial t} = \sigma_{S_0}\left(\frac{d}{r}\right) - \mu_{S_0}S_0 + D_{S_0}\Delta S_0 \qquad (1)$$

where σ_{S_0} is the basic production rate, r is the radius of the domain and D_{S_0} is the diffusion coefficient. Cells that have an S_0 concentration lower than a threshold value (S_0^*) trigger the production of a specific diffusible signal S_1, while concentrations that are
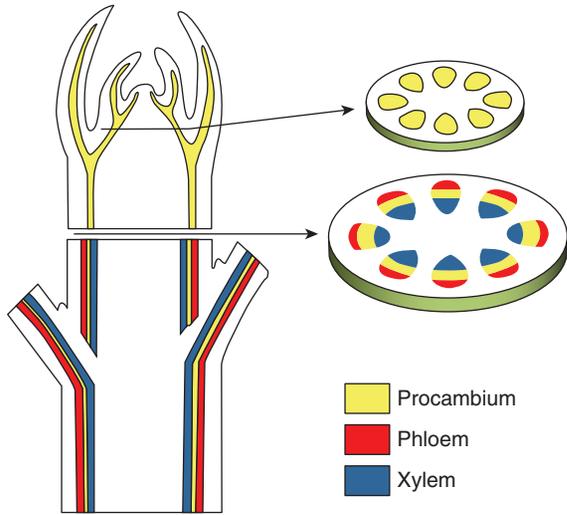
FIG. 1. Schematic representation of a typical arrangement of vascular tissues in plants.

higher or equal to S_0^* trigger the production of another specific diffusible signal S_2 (Fig. 2A).

Procambium. The differentiation of procambium is formulated as an activator–substrate system (Meinhardt, 1982) describing the dynamics of two diffusible substrates and one diffusible autocatalytic activator. Signals S_1 and S_2 have the role of substrates (i.e. S can be read as 'signal' and 'substrate' interchangeably) and they are both consumed to promote the autocatalytic reaction of the procambium activator A_P (Fig. 2B). The system is written as:

$$\frac{\partial S_1}{\partial t} = \overline{\sigma_{S_1}}\left(1 - \frac{S_1}{1 + k_S A_P}\right) - \rho_S A_P^2 S_1 S_2 + D_S \Delta S_1 \quad (2)$$

$$\frac{\partial S_2}{\partial t} = \overline{\sigma_{S_2}}\left(1 - \frac{S_2}{1 + k_S A_P}\right) - \rho_S A_P^2 S_1 S_2 + D_S \Delta S_2 \quad (3)$$

$$\frac{\partial A_P}{\partial t} = \sigma_{A_P} + \rho_{A_P} A_P^2 S_1 S_2 + \mu_{A_P} A_P + D_{A_P} \Delta A_P \quad (4)$$

where $\overline{\sigma_{S_1}}$ and $\overline{\sigma_{S_2}}$ are spatially variable parameters defined as follows:

$$\overline{\sigma_{S_1}} = \begin{cases} \sigma_S, & S_0 < S_0^* \\ 0, & S_0 \geq S_0^* \end{cases}$$
$$\overline{\sigma_{S_2}} = \begin{cases} 0, & S_0 < S_0^* \\ \sigma_S, & S_0 \geq S_0^* \end{cases}$$

and σ_S is the basic production rate of the two substrates that are specifically produced in different conditions: S_1 is produced only in the central domain ($S_0 < S_0^*$) and S_2 only in the peripheral domain ($S_0 \geq S_0^*$); σ_{A_P} is the basic production rate of the procambium activator; k_S is the saturation constant of the substrate's production; ρ_S and ρ_{A_P} are the cross-reaction coefficients; μ_{A_P} is the removal rate of A_P; and D_S and D_{A_P} are the diffusion coefficients. If the concentration of A_P is higher than or equal to the threshold value A_P^*, this triggers the differentiation of procambium (Fig. 2C).
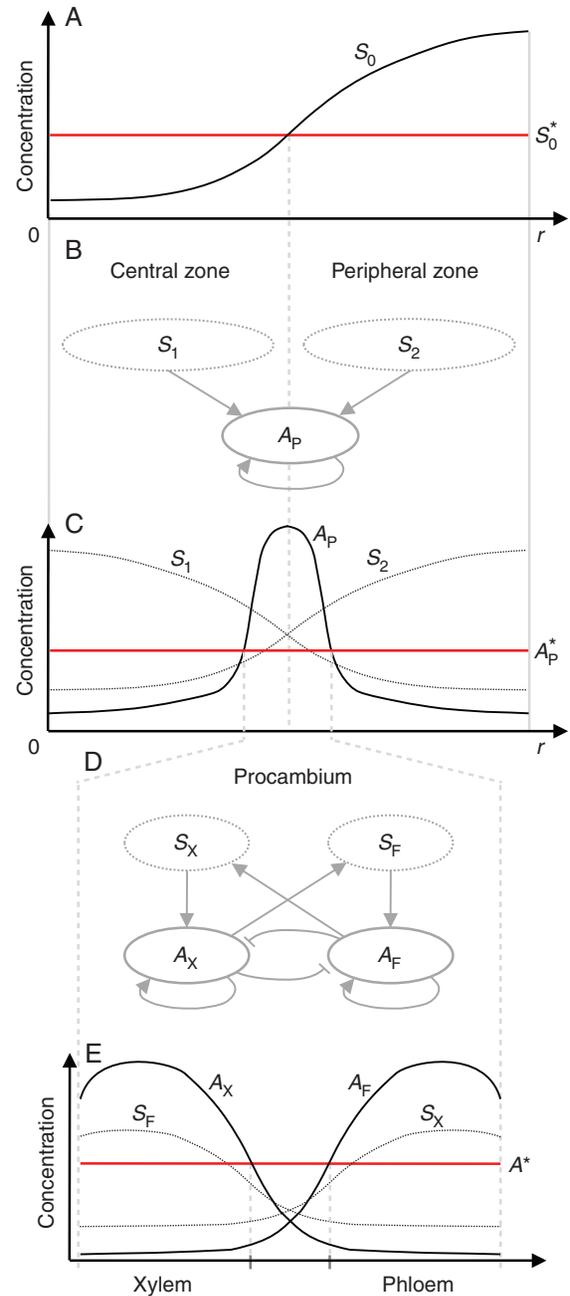
FIG. 2. Schematic representation of model processes. (A) Steady-state profile of the S_0 concentration along the section radius. Central and peripheral zones are defined according to S_0^*. (B) Procambium substrate–activator dynamics described by eqns (2)–(4). (C) Steady-state profile of S_1, S_2 and A_P along the radius of a simulated plant section. The A_P peak is established at the boundary between the central and peripheral zones as an emergent property of both S_1 and S_2 concentration gradients. Procambium is differentiated where A_P is above the threshold value A_P^*. (D) Xylem and phloem activator dynamics described by eqns (5)–(9). (E) Steady-state profile of xylem and phloem activators (A_X and A_F) and substrates (S_X and S_F) within a procambial strand.

Phloem and xylem. The differentiation of phloem and xylem vascular tissues is described by the dynamics of two autocatalytic activators (A_F and A_X, promoting the differentiation of phloem and xylem, respectively) that exclude each other locally through the production of a common repressor R, but mutually

activate each other over a long range via the production of each other's substrate (S_F and S_X). Moreover, facilitation of phloem in the peripheral zone and xylem in the central zone is considered (Fig. 2D). The equations are formulated, based on Meinhardt and Gierer (1980), as follows:

$$\frac{\partial A_F}{\partial t} = \overline{Pro}\left(\sigma_{A_{XF}} + \rho_{A_{XF}}\frac{A_F^2 S_F}{1+R}\right) - \mu_{A_{XF}}A_F + D_{A_F}\Delta A_F \quad (5)$$

$$\frac{\partial A_X}{\partial t} = \overline{Pro}\left(\sigma_{A_{XF}} + \rho_{A_{XF}}\frac{A_X^2 S_X}{1+R}\right) - \mu_{A_{XF}}A_X + D_{A_X}\Delta A_X \quad (6)$$

$$\frac{\partial S_F}{\partial t} = \overline{Pro}\left[\overline{\sigma_{S_F}} + \gamma_{S_{XF}}(A_X - S_F)\right] - \mu_{S_{XF}}S_F + D_{S_{XF}}\Delta S_F \quad (7)$$

$$\frac{\partial S_X}{\partial t} = \overline{Pro}\left[\overline{\sigma_{S_X}} + \gamma_{S_{XF}}(A_F - S_X)\right] - \mu_{S_{XF}}S_X + D_{S_{XF}}\Delta S_X \quad (8)$$

$$\frac{dR}{dt} = \rho_{A_{XF}}A_F^2 S_F + \rho_{A_{XF}}A_X^2 S_X - \mu_R R \quad (9)$$

where $\overline{Pro}$ is a spatially variable parameter defined as:

$$\overline{Pro} = \begin{cases} 0, & A_P < A_P^* \\ 1, & A_P \geq A_P^* \end{cases}$$

meaning that the substances in eqns (5)–(9) are only produced and react within differentiated procambial cells ($A_P \geq A_P^*$). Two more spatially variable parameters, $\overline{\sigma_{S_F}}$ and $\overline{\sigma_{S_X}}$, are included to define the local facilitation of phloem and xylem activation. Here we assume the promotion of phloem over the peripheral zone and of xylem over the central zone, defined as follows:

$$\overline{\sigma_{S_F}} = \begin{cases} 0, & S_0 < S_0^* \\ \sigma_{S_{XF}}, & S_0 \geq S_0^* \end{cases}$$

$$\overline{\sigma_{S_X}} = \begin{cases} \sigma_{S_{XF}}, & S_0 < S_0^* \\ 0, & S_0 \geq S_0^* \end{cases}$$

$\sigma_{A_{XF}}$ and $\sigma_{S_{XF}}$ are the basic production rates, $\rho_{A_{XF}}$ and $\gamma_{S_{XF}}$ are the reaction coefficients, $\mu_{A_{XF}}$, $\mu_{S_{XF}}$ and μ_R are the removal rates, and D_{A_F}, D_{A_X} and $D_{S_{XF}}$ are the diffusion coefficients. If the concentration of either A_F or A_X is higher than or equal to the threshold value A^*, this triggers the differentiation into phloem or xylem, respectively (Fig. 2E).

Figure 2 graphically explains the general behaviour of all three parts of the model. Moreover, Supplementary Data Figure S1 shows the diagram of the model steps leading to the differentiation of vascular tissues from the point of view of a single cell.

Numerical simulations

All numerical calculations were implemented in MATLAB R2012b (MathWorks Inc.) and the reaction–diffusion dynamics were integrated using the Euler method. The simulations were carried out for a total time $T = 20\,000$ (and a time step

TABLE 1. *List of parameters and simulation values of eqns (1)–(4)*

Parameter	Description	Value
σ_{S_0}	S_0 basic production rate	0·012
r	Radius of the domain	20; 40
d	Distance from centre of the domain	$[0\ r]$
μ_{S_0}	S_0 consumption rate	0·015
D_{S_0}	S_0 diffusion coefficient	0·8
σ_S	S basic production rate	0·04
k_S	S production saturation constant	20
ρ_S	S cross-reaction coefficient	0·08
D_S	S diffusion coefficient	0·5
σ_{A_P}	A_P basic production rate	0·001
ρ_{A_P}	A_P cross-reaction coefficient	0·03; 0·05
μ_{A_P}	A_P removal rate	0·02
D_{A_P}	A_P diffusion coefficient	0·02
S_0^*	Threshold value for definition of central/peripheral zones	0·5
A_P^*	Threshold value for differentiation of procambium	0·5

TABLE 2. *List of parameters and simulation values of eqns (5)–(9)*

Parameter	Description	Value
$\sigma_{A_{XF}}$	A_F and A_X basic production rate	0·01
$\rho_{A_{XF}}$	A_F and A_X cross-reaction coefficient	0·1
$\mu_{A_{XF}}$	A_F and A_X removal rate	0·01
D_{A_F}	A_F diffusion coefficient	0·001–0·003
D_{A_X}	A_X diffusion coefficient	0·001–0·003
$\sigma_{S_{XF}}$	S_F and S_X basic production rate	0·001
$\gamma_{S_{XF}}$	S_F and S_X reaction coefficient	0·03
$\mu_{S_{XF}}$	S_F and S_X removal rate	0·01
$D_{S_{XF}}$	S_F and S_X diffusion coefficient	0·02
μ_R	R removal rate	0·5
A^*	Threshold value for differentiation of phloem and xylem	30

$dt = 0\cdot1$) or until the steady state was reached. The plant section, i.e. the spatial domain equations, was set as a circular lattice with zero-flux Neumann boundary conditions and radius r (number of pixels). The initial value of all state variables was set to zero. Tables 1 and 2 contain the list of all parameters and the values used in numerical simulations. For simplicity, no domain growth was considered during the simulations.

The model analysis has been performed through a series of numerical simulations:

(1) The definition of central and peripheral zones has been tested in relation to section radius r.
(2) The emergence of procambial spatial patterns has been assessed in relation to the change of two parameters: section radius r and procambium cross-reaction coefficient ρ_{A_P}.
(3) Starting from different arrangements of procambium, the effects of A_F and A_X diffusion coefficients (D_{A_F} and D_{A_X}) on the emergent patterns of phloem and xylem were tested.

A qualitative comparison between simulated patterns and observed vascular arrangements (as classified by Beck *et al.*, 1980) was carried out.
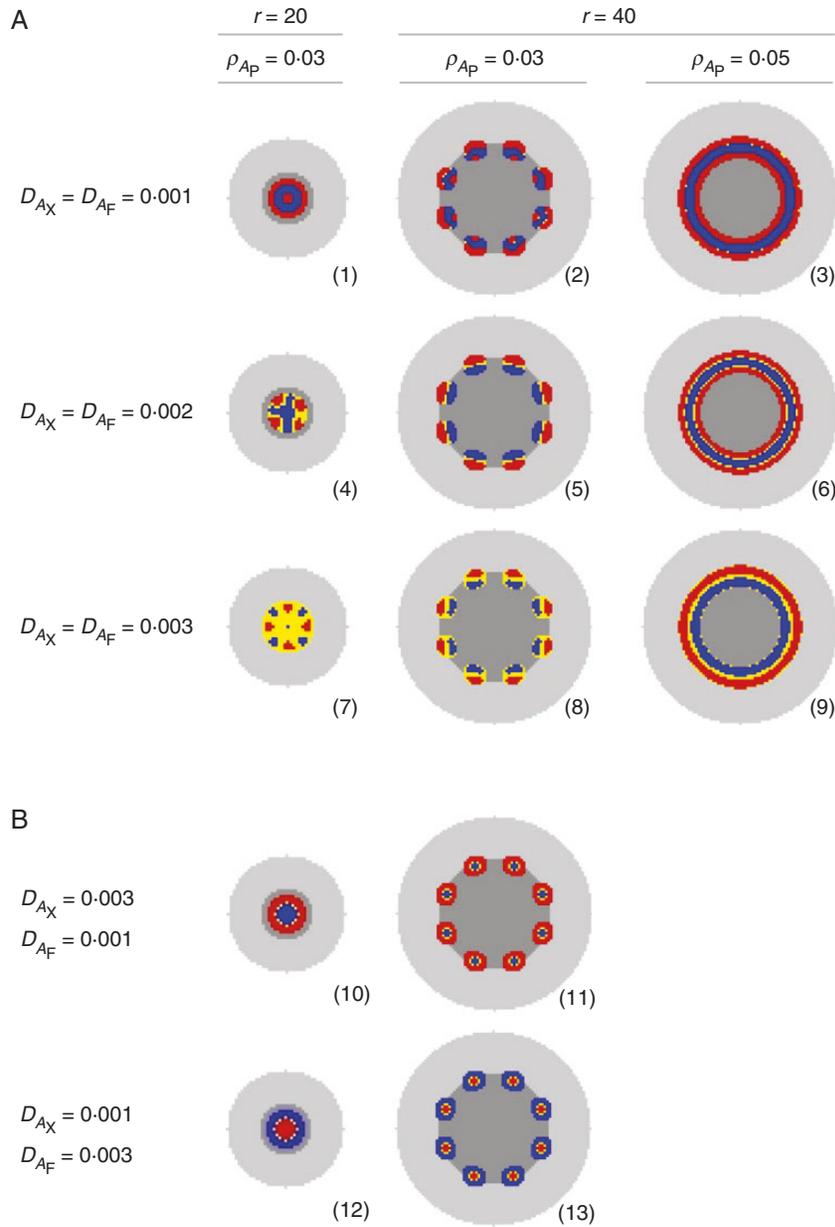
RESULTS

Definition of central and peripheral zones

The simple diffusive processes described by eqn. (1) produce a rapid change of the concentration of S_0, which reaches the steady state with a concentration gradient along the radius (Fig. 2A), with a maximum at the boundary of the domain and a minimum at the centre. For values of the radius $r > 10$, eqn (1) consistently produces two distinct zones, one internal with $S_0 < S_0^*$ and one external with $S_0 \geq S_0^*$, while for values of the radius $r \leq 10$, the concentration of S_0 was found to be higher than S_0^* in all the domains, thus failing to produce the internal zone (simulations not shown).

Procambium differentiation

The emergent spatial pattern of procambium differentiation was found to be highly dependent on the cross-reaction coefficient of the procambium activator (ρ_{A_P}) and the radius of the simulated spatial domain (r). As shown in Fig. 3, no procambium is differentiated for low reaction coefficients ($\rho_{A_P} \leq 0.020$) or for very small sections ($r \leq 10$). In the first case, no peaks of A_P may be established due to the insufficient conversion of the substrates into activator, while in the second case the production of A_P cannot start due to the absence of substrate S_1 production because of the concentration gradient of S_0 (see previous section). A protostelic structure (P) consistently emerges for domains with a radius <30, while, for higher radii, either eustelic (E) or siphonostelic (S) patterns emerge, clearly depending on parameter ρ_{A_P}. The eustele and siphonostele structures differentiate for low and high values of ρ_{A_P}, respectively. Interestingly, for values of ρ_{A_P} of around 0.038, an intermediate pattern

between eustele and protostele emerges (SE in Fig. 3), where isolated spots arranged in an eustelic pattern are still connected by a continuous thin ring of procambial cells.

The increase in the cross-reaction coefficient ρ_{A_P} resulted in a shift from a spotted to a striped pattern, which is in agreement with the work on activator–substrate systems by Meinhardt (1982). The striped pattern assumes a ring shape due to the emergent property of the positioning of activator peaks. Activator autocatalysis needs two substrates that are produced in distinct areas. For this reason A_P peaks tend to form at the boundary between the two areas, i.e. where both substrates are most available. As the domain size decreases, spots or stripes that are usually segregated begin to form closer to one another until they merge together, forming a single spot in the centre of the domain ($r \leq 30$). Such protostelic structures are typically found in roots of most plant species and also in some stems, particularly of primitive species.

Other parameters such as the diffusion coefficients (D_{A_P} and D_S) were found to have no effect on the type of pattern generated, but rather were related to other features such as the width of A_P peaks, i.e. the width of procambium spots and rings (simulations not shown).

Phloem and xylem differentiation

In the second simulated experiment (Fig. 4), we tested the effects of both the diffusion coefficients of phloem and xylem activators (D_{A_X} and D_{A_F}) and the starting spatial configuration of procambium (depending on ρ_{A_P} and r) on phloem and xylem differentiation patterns. The diffusion coefficients were progressively increased, in a factorial combination, from 0.001 up to 0.003. In general, as the diffusion coefficients increase, so does

Fig. 3. Effects of radius r and cross-reaction coefficient ρ_{A_P} on procambium differentiation patterns. A protostelic structure (P) is formed for domains with a radius <30, while, for higher radii, eustelic (E) and siphonostelic (S) patterns emerge. An intermediate pattern between siphonostele and eustele (SE) emerges for values of ρ_{A_P} of around 0.038. Other parameter values are listed in Table 1. See text for details.

FIG. 4. Effect of diffusion coefficients D_{A_X} and D_{A_F} and procambium configuration on xylem and phloem differentiation patterns. Other parameter values are listed in Tables 1 and 2. See text for details.

the width of the activators peaks. According to this, with $D_{A_X} = D_{A_F} = 0.001$, a central band of xylem is formed surrounded by phloem on both the inside and the outside, generating three easily recognizable structures: amphiphloic protostele (Fig. 4, section 1); eustele with bicollateral bundles (Fig. 4, section 2); and amphiphloic siphonostele (Fig. 4, section 3). With $D_{A_X} = D_{A_F} = 0.002$, the size of activators peaks start to increase and so does the competition for space, creating two more distinct patterns: actinostele (Fig. 4, section 4) with spots of phloem on the outside of the vascular strand with internal star-shaped xylem; and eustele with collateral bundles (Fig. 4, section 5; Supplementary Data Video S1). Similarly, for $D_{A_X} = D_{A_F} = 0.003$, a protostele with mixed phloem and xylem (Fig. 4, section 7) and an ectophloic siphonostele (Fig. 4, section 9;

Supplementary Data Video S2) are formed. Interestingly, for decoupled values of the diffusion coefficients ($D_{A_X} \neq D_{A_F}$), every single vascular bundle differentiates with one tissue type completely surrounded by the other. In particular, the one with the higher diffusion coefficient consistently occupies the central position and four new observed structures are produced by simulations: ectophloic (Fig. 4, section 10) and endophloic (Fig. 4, section 12) protostele; and eustele with amphicribral (Fig. 4, section 11) and amphivasal (Fig. 4, section 13) bundles.

DISCUSSION

Since the beginning of the 20th century, increasing attention to the anatomical structure of vascular tissues in plants from
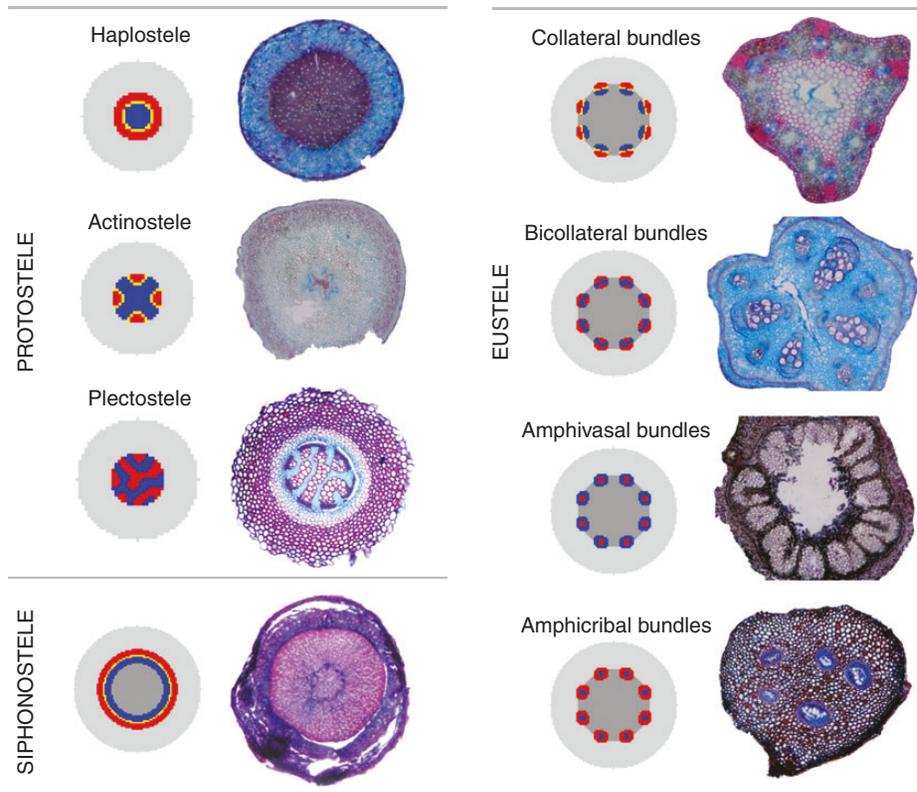
FIG. 5. Spatial patterns of vascular tissues in both simulated and observed plant transverse sections. Haplostele: *Mespilus germanica* root. Actinostele: *Psilotum nudum* stem. Plectostele: *Lycopodium annotinum* stem. Siphonostele: *Mespilus germanica* stem. Eustele with collateral bundles: *Carex glareosa* stem. Eustele with bicollateral bundles: *Cucumis sativa* stem. Eustele with amphivasal bundles: *Osmunda regalis* stem. Eustele with amphicribal bundles: *Dryopteris robertiana* stem.

evolutionary and developmental points of view is found in the botanical literature (e.g. Worsdell, 1902; Jeffrey, 1903). In the following decades, the focus shifted from macro- and microscopic studies of anatomical features to the investigation of genetic and physiological aspects of vascular differentiation (Sieburth *et al.*, 2006).

A large number of experimental studies, mainly on model plants such as arabidopsis, *Zinnia* and *Populus*, reported on plant hormonal control of vascular development. Auxin, in particular, has been considered for its wide-ranging influence on several aspects of development, e.g. promoting cell division (Schrader *et al.*, 2004), inducing the differentiation of xylem tracheary elements (Yoshida *et al.*, 2009), and formation and maintenance of vascular continuity along plant organs through its polar transport (Scarpella *et al.*, 2006). Brassinosteroid was also found to play a role in promotion of cell expansion and vascular development (Vert and Chory, 2006). Cytokinin was found to regulate protoxylem specification negatively in arabidopsis (Mähönen *et al.*, 2006). Many transcriptional regulators implicated in vascular cell specification have recently been identified. For example, MP is an auxin-responsive transcriptional activator, belonging to the family of auxin response factors (ARFs), that regulates the specification of procambial cells via the induction of expression of *ATHB-8* (Donner *et al.*, 2009).

Most experimental studies focused on different specific aspects of the vascular development of plants; however, the interactions between the system components still need to be clarified in terms of both their spatial and temporal processes. Recent modelling work by Muraro *et al*. (2014) showed the possibility of effectively simulating the molecular networks involved in xylem and procambium specification and their radial patterning. The authors developed a mathematical model incorporating auxin and cytokinin signalling networks and transport dynamics to test whether their mutually inhibitory interactions can explain vascular patterning. In particular, they were able to show that the restriction of *PHB* by miRNA165/166 is necessary for the establishment of the arabidopsis root bisymmetric pattern and also that an unidentified component of the network is required to account for the spatial expression of *ARR5*.

The aim of our work was to investigate the spatial and temporal processes involved in vascular patterning that could also account for the diversity of steles observed in nature. We thus formulated a general modelling framework based on the reaction–diffusion systems proposed by Turing (1953) and applied by Meinhardt (1982) to animal and plant development.

The main feature of the proposed model is its ability to simulate developmental processes dynamically as different integrated modules. Moreover, the simplicity of the formulation allowed for the recognition of a limited number of parameters generating different emerging patterns of both procambium within the plant section, and phloem and xylem within each bundle. Simulation results showed that the model was capable of reproducing most vascular spatial patterns observed in plants, from primitive and simple structures, consisting of a single strand of vascular

bundles (protostele), to more complex and evolved structures, with separated vascular bundles arranged in an ordered pattern within the plant section. An interesting result is the formation of the protostele for small simulation domains. This result seems to be consistent with the occurrence of this particular structure in species and organs with relatively smaller dimensions which are typically found in primitive plants (e.g. Pteridophyta). It is noteworthy that apical meristems in roots are generally smaller than in shoots and the usual root vascular arrangement is the atactostele where peripheral spots of phloem are surrounded by internal xylem (Esau, 1977). Figure 5 summarizes such results showing representative comparative examples between simulated patterns and transverse sections of different species.

All the reported patterns were determined under the assumption that phloem and xylem are specifically promoted in the peripheral and central zones, respectively. As already mentioned, this assumption reflects the experimental evidence suggested by genetic analyses on arabidopsis whereby genes involved in the specification of adaxial–abaxial (central–peripheral) polarity are also responsible for specification of phloem and xylem. We also investigated two different cases, i.e. the opposite facilitation condition (with phloem and xylem promoted in the central and peripheral zone, respectively) and the case of complete absence of local facilitation. Interestingly, some spatial patterns were found to be completely insensitive to facilitation, in particular those that emerged due to differences in the diffusion coefficients of the phloem and xylem activators (Fig. 4B). On the one hand, when opposed local facilitation was assumed, the radial patterns of phloem and xylem simply turned out to be inverted (data not shown). On the other hand, when no facilitation of the two activators was implemented ($\overline{\sigma_{S_F}} = \overline{\sigma_{S_X}} = 0$), the simulations generated an arrangement where phloem and xylem form alternated bands, a structure called plectostele (see Fig. 5) that is found, for instance, in plants of the genus *Lycopodium*.

Another important structure, typical of the monocots, is the atactostele, generally defined as a 'system of randomly scattered bundles', whereas it is clear that the system components have a specific and predictable behaviour (Beck *et al.*, 1982). In monocotyledonous seedlings, the vascular system is arranged in a central cylinder very similar to that of dicotyledons (Tomlinson, 1970). Afterwards, peripheral stem bundles originate from the discs of leaf insertion, where the midvein and secondary veins develop both acropetally through the leaf lamina and basipetally into the stem where they eventually connect with the stem vasculature (Nelson and Dengler, 1997). For such reasons, the presented model is in agreement with the development of vascular bundles also in monocots where the first and innermost set of bundles develops as a typical eustelic pattern and the formation of new leaves leads to the insertion of new veins within the stem, resulting in the final observed pattern (Supplementary Data Fig. S2).

In conclusion, the model showed the capability to reproduce qualitatively the most diverse radial arrangements of vascular tissues. Future work could involve performing a systematic comparison of our simulations with a more extensive set of observed patterns to verify, for instance, the prediction of structures not (yet) found in nature and to investigate the occurrence of the protostele in correlation to meristem size. Moreover, the model could be applied for comparative analysis with arabidopsis mutants which show aberrant vascular patterns to better understand the relationships between specific gene functionality and anatomical development.

SUPPLEMENTARY DATA

Supplementary data are available online at www.aob.oxford journals.org and consist of the following. Figure S1: diagram of the model steps leading to the differentiation of vascular tissues from the point of view of a single cell. Figure S2: schematic representation of the formation of the atactostele. Video S1: simulation run producing the eustele vascular arrangement. Video S2: simulation run producing the siphonostele vascular arrangement.

ACKNOWLEDGEMENTS

LITERATURE CITED

Bayer E, Smith R, Mandel T, *et al*. 2009. Integration of transport-based models for phyllotaxis and midvein formation. *Genes and Development* **23**: 373–384.

Beck CB, Schmidt R, Rothwell GW. 1982. Stelar morphology of the primary vascular system of seed plants. *Botanical Review* **48**: 691–815.

Bishopp A, Help H, El-Showk S, *et al*. 2011*a*. A mutually inhibitory interaction between auxin and cytokinin specifies vascular pattern in roots. *Current Biology* **21**: 917–926.

Bishopp A, Lehesranta S, Vaten A, *et al*. 2011*b*. Phloem-transported cytokinin regulates polar auxin transport and maintains vascular pattern in the root meristem. *Current Biology* **21**: 927–932.

Blilou I, Xu J, Wildwater M, *et al*. 2005. The PIN auxin efflux facilitator network controls growth and patterning in *Arabidopsis* roots. *Nature* **433**: 39–44.

Bonke M, Thitamadee S, Mähönen AP, Hauser MT, Helariutta Y. 2003. APL regulates vascular tissue identity in *Arabidopsis*. *Nature* **426**: 181–86.

Bowman JL, Floyd SK. 2008. Patterning and polarity in seed plant shoots. *Annual Review of Plant Biology* **59**: 67–88.

Caño-Delgado A, Lee JY, Demura T. 2010. Regulatory mechanisms for specification and patterning of plant vascular tissues. *Annual Review of Cell and Developmental Biology* **26**: 605–637.

Carlsbecker A, Helariutta Y. 2005. Phloem and xylem specification: pieces of the puzzle emerge. *Current Opinion in Plant Biology* **8**: 512–517.

Donner TJ, Sherr I, Scarpella E. 2009. Regulation of preprocambial cell state acquisition by auxin signaling in *Arabidopsis* leaves. *Development* **136**: 3235–3246.

Emery JF, Floyd SK, Alvarez J, *et al*. 2003. Radial patterning of *Arabidopsis* shoots by class III HD-ZIP and KANADI genes. *Current Biology* **13**: 1768–1774.

Esau K. 1977. *Anatomy of seed plants*. New York: Wiley.

Eshed Y, Baum SF, Perea JV, Bowman JL. 2001. Establishment of polarity in lateral organs of plants. *Current Biology* **11**: 1251–1260.

Eveland AL, Jackson DP. 2012. Sugars, signalling, and plant development. *Journal of Experimental Botany* **63**: 3367–3377.

Feugier FG, Mochizuki A, Iwasa Y. 2005. Self-organization of the vascular system in plant leaves: inter-dependent dynamics of auxin flux and carrier proteins. *Journal of Theoretical Biology* **236**: 366–375.

Fujita H, Toyokura K, Okada K, Kawaguchi M. 2011. Reaction–diffusion pattern in shoot apical meristem of plants. *PLoS One* **6**: e18243.

Hardtke CS, Berleth T. 1998. The *Arabidopsis* gene MONOPTEROS encodes a transcription factor mediating embryo axis formation and vascular development. *EMBO Journal* **17**: 1405–1411.

Ilegems M, Douet V, Meylan-Bettex M, *et al*. 2010. Interplay of auxin, KANADI and Class III HD-ZIP transcription factors in vascular tissue formation. *Development* **137**: 975–984.

Jeffrey EC. 1903. The structure and development of the stem in the Pteridophyta and Gymnosperms. *Philosophical Transactions of the Royal Society B: Containing Papers of a Biological Character* **195**: 119–146.

Jönsson H, Krupinski P. 2010. Modeling plant growth and pattern formation. *Current Opinion in Plant Biology* **13**: 5–11.

Jönsson H, Gruel J, Krupinski P, Troein C. 2012. On evaluating models in computational morphodynamics. *Current Opinion in Plant Biology* **15**: 103–110.

Kerstetter R, Bollman K, Taylor R, Bomblies K, Poethig R. 2001. *KANADI* regulates organ polarity in *Arabidopsis*. *Nature* **411**: 706–709.

Mähönen AP, Bishopp A, Higuchi M, *et al*. 2006. Cytokinin signaling and its inhibitor AHP6 regulate cell fate during vascular development. *Science* **311**: 94–98.

Meinhardt H. 1982. *Models of biological pattern formation*. London: Academic Press.

Meinhardt H, Gierer A. 1980. Generation and regeneration of sequences of structures during morphogenesis. *Journal of Theoretical Biology* **85**: 429–450.

Mitchison GJ. 1980. A model for vein formation in higher plants. *Proceedings of the Royal Society B: Biological Sciences* **207**: 79–109.

Muraro D, Mellor N, Pound MP, *et al*. 2014. Integration of hormonal signaling networks and mobile microRNAs is required for vascular patterning in *Arabidopsis* roots. *Proceedings of the National Academy of Sciences, USA* **111**: 857–862.

Nelson T, Dengler NG. 1997. Leaf vascular pattern formation. *The Plant Cell* **9**: 1121–1135.

Pien S, Wyrzykowska J, Fleming AJ. 2001. Novel marker genes for early leaf development indicate spatial regulation of carbohydrate metabolism within the apical meristem. *The Plant Journal* **25**: 663–674.

Prusinkiewicz P, Runions A. 2012. Computational models of plant development and form. *New Phytologist* **193**: 549–569.

Sachs T. 1969. Polarity and the induction of organized vascular tissues. *Annals of Botany* **33**: 263–275.

Scarpella E, Marcos D, Friml J, Berleth T. 2006. Control of leaf vascular patterning by polar auxin transport. *Genes and Development* **20**: 1015–1027.

Schrader J, Nilsson J, Mellerowicz E, *et al*. 2004. A high-resolution transcript profile across the wood-forming meristem of poplar identifies potential regulators of cambial stem cell identity. *The Plant Cell* **16**: 2278–2292.

Sieburth LE, Deyholos MK. 2006. Vascular development: the long and winding road. *Current Opinion in Plant Biology* **9**: 48–54.

Teale WD, Paponov IA, Palme K. 2006. Auxin in action: signalling, transport and the control of plant growth and development. *Nature Reviews Molecular Cell Biology* **7**: 847–859.

Tomlinson PB. 1970. Monocotyledons – towards an understanding of their morphology and anatomy. *Advances in Botanical Research* **3**: 207–292.

Turing AM. 1953. The chemical basis of morphogenesis. *Bulletin of Mathematical Biology* **52**: 153–197.

Vanstraelen M, Benková E. 2012. Hormonal interactions in the regulation of plant development. *Annual Review of Cell and Developmental Biology* **28**: 463–487.

Vert G, Chory J. 2006. Downstream nuclear events in brassinosteroid signaling. *Nature* **441**: 96–100.

Waites R, Selvadurai HR, Oliver IR, Hudson A. 1998. The PHANTASTICA gene encodes a MYB transcription factor involved in growth and dorsoventrality of lateral organs in Antirrhinum. *Cell* **93**: 779–789.

Wilson W. 1978. The position of regenerating cambia: auxin/sucrose ratio and the gradient induction hypothesis. *Proceedings of the Royal Society B: Biological Sciences* **203**: 153–176.

Worsdell WC. 1902. The evolution of the vascular tissues of plants. *Botanical Gazette* **34**: 216–223.

Yoshida S, Iwamoto K, Demura T, Fukuda H. 2009. Comprehensive analysis of the regulatory roles of auxin in early transdifferentiation into xylem cells. *Plant Molecular Biology* **70**: 457–69.